



Cosmic shear on small angular scales from the WFPC2 Archival Parallels

Yogesh Wadadekar, Stefano Casertano, Henry C. Ferguson and Andrew Fruchter

STScI, 3700 San Martin Drive, Baltimore MD 21218

ABSTRACT: We present a preliminary characterization of data from the WFPC2 archival parallels project that we plan to use for a measurement of the weak lensing cosmic shear. The data we are considering cover about 1.5 sq. degrees in about 1100 pointings, in the F606W filter. At typical exposure times of 1000s to 5000s per pointing, we detect 30-60 galaxies per square arcmin. This dataset is nearly 4 times larger than the largest previously used WFPC2 dataset and will allow us to probe cosmic shear from 2 arcmin to 10 arcsec marking the transition from linear to non-linear structure growth at redshift ~ 1 . We are currently implementing a moment-based technique; shapelet based techniques will be explored in the near future. We employ a combination of on-orbit measurements and simulations to account for the effects of geometric distortion and the PSF.

The data: WFPC2 Archival Parallels

We use data from the WFPC2 Archival Parallels (Wadadekar et. al 2006; APPP). The APPP uses state-of-the-art tools to combine about 10,000 WFPC2 parallel datasets to produce combined, drizzled, astrometrically registered, background offset corrected, cosmic-ray cleaned images and associated weight files using a custom developed pipeline (see Fig. 1). Updated WCS coordinates for each of the WFPC2 chips are available as a product of the accurate image registration. A majority of the APPP images are in the F606W filter at galactic latitude > 20 deg. along ~ 1100 random lines of sight, thus reducing the sampling (cosmic) variance (Fig. 2). The area coverage and the depth of the data are expected to be sufficient for a measurement of cosmic shear on angular scales of 2 arcmin to 20 arcsec and possibly 10 arcsec. We use SExtractor (version 2.4.3) for source detection over the three WF chips, excluding the chip edges. We combine information from SExtractor's star/galaxy classification and additional derived parameters to separate our sources into stars and galaxies. With additional constraints on S/N and on SExtractor FLAGS, we obtain a sample of 203,000 galaxies with $21 < V < 26$ which form our primary sample. A subset of these will be used for the final shear measurement.

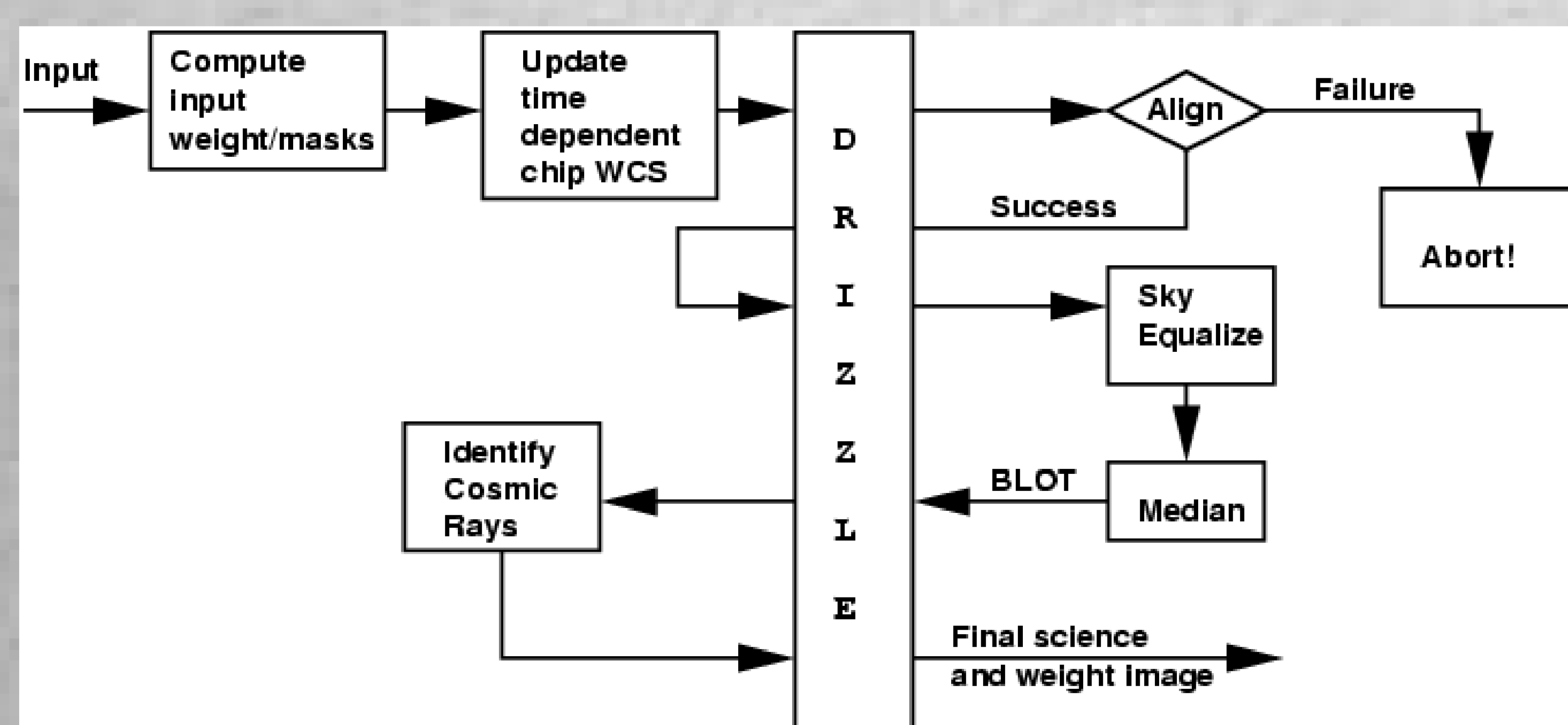


Fig. 1: Data flow diagram for the drizzle based pipeline developed for APPP data processing. Special attention is paid to image registration and sky background equalization.

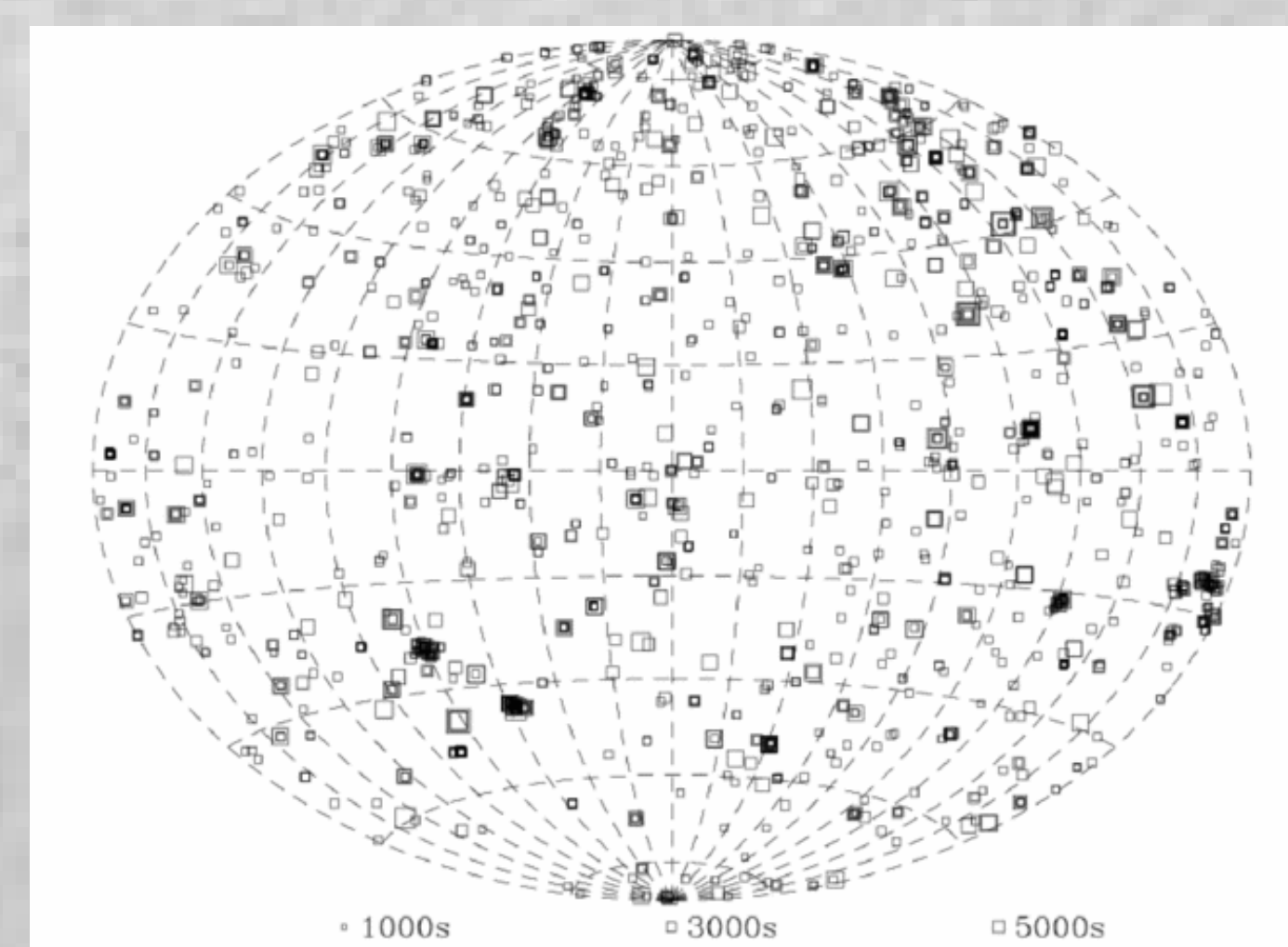


Fig. 2: Distribution of APPP datasets on the sky in galactic coordinates. Datasets at high galactic latitude located away from known clusters will be used for the shear measurement.

Shear Measurement technique

The diversity and limitations of the APPP data require special care in the shape measurements that form the basis of the cosmic shear analysis. Unlike targeted programs, the data cover a broad range of total exposure time, number of exposures, dithering patterns, telescope focus, and position in the sky. Because of this diversity and the total size of our dataset, the largest set of WFPC2 images ever used in a cosmic shear study, we will be especially sensitive to small residual systematics in the data and/or analysis. Therefore, we plan to reconsider several types of potential systematics and use two independent methods to determine object shapes: the moment-based technique of Rhodes et al. (2000), which adapts to WFPC2 data the method developed by Kaiser et al (1995); and the implementation developed by Park et al. (2004) of the Laguerre expansion (polar shapelet) method introduced by Bernstein & Jarvis (2002). The preliminary work presented here refers to our initial tests and verification of the Rhodes et al technique. In particular, we present measurements of both synthetic (TinyTim, Krist and Burrows 1995) and observed point sources, in order to illustrate the impact of detector properties, telescope focus, and subpixel placement on the measured shapes of pure point-spread functions.

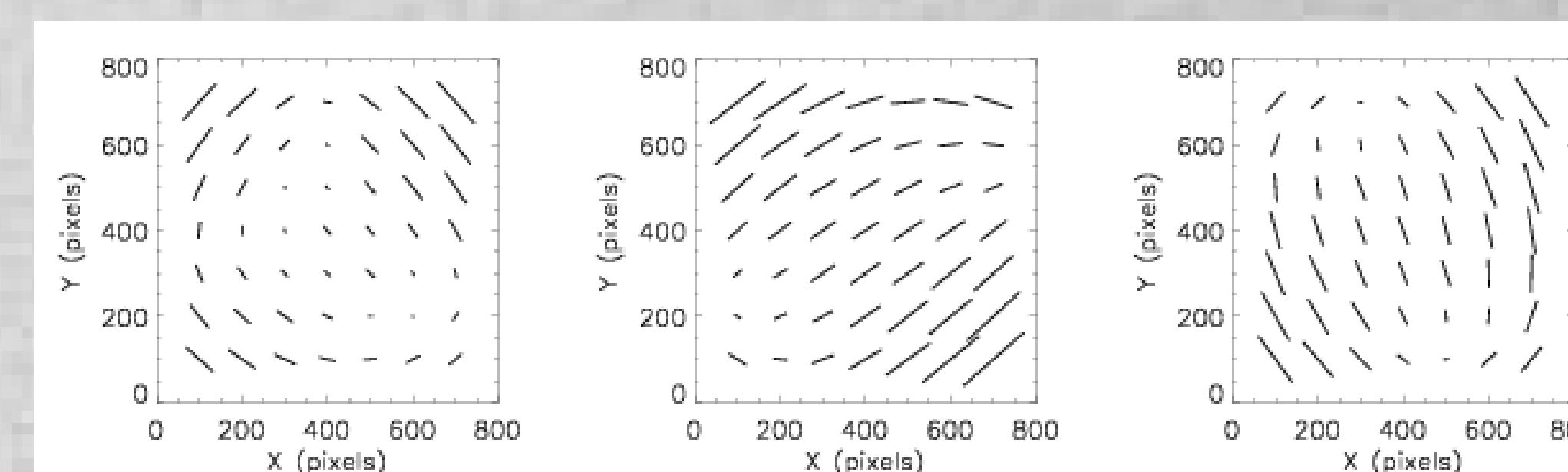


Fig.3 PSF ellipticity predicted by TinyTim, for WF2,WF3 and WF4, for a focus value of 0 microns. The camera distortion is not included. The ellipticities are scaled up by a factor of 400.

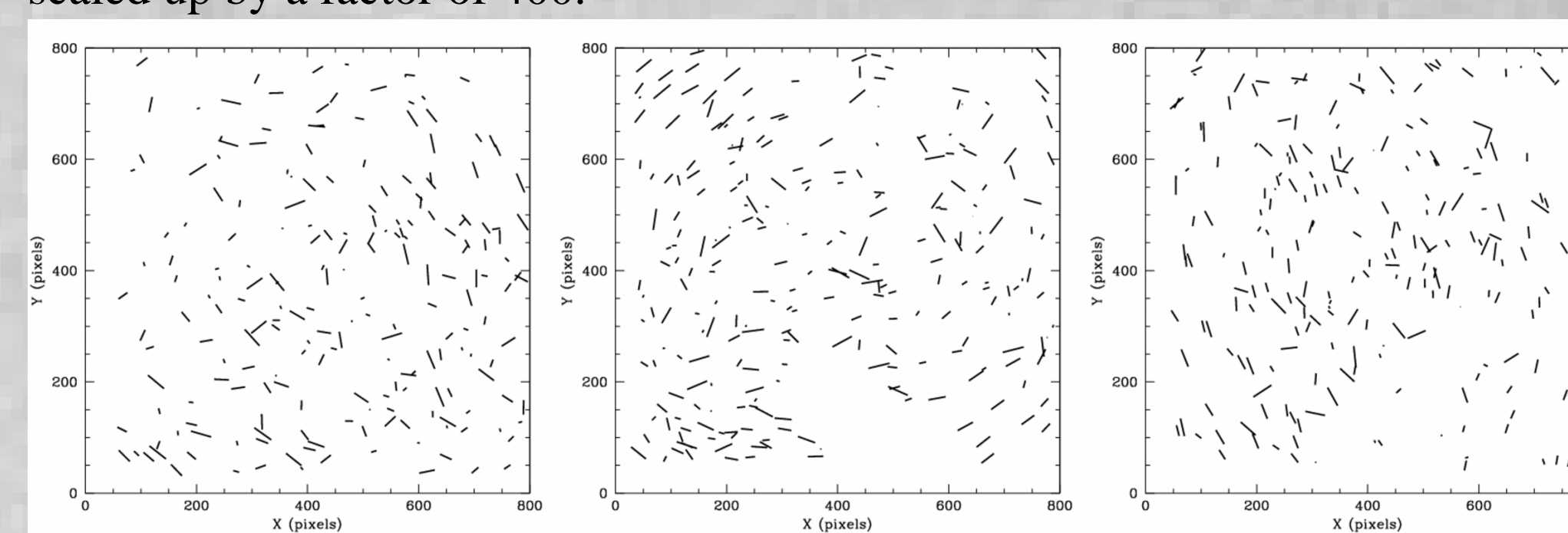


Fig. 4 Ellipticity values measured with real stellar images from a field in the LMC for the three WF chips. These measures include the camera distortion and have been scaled by a factor of 200.



Fig. 5: BVI color composite of an APPP field in the LMC. One F606W image from this pointing was used for the PSF measurement shown in Fig. 4. Data from fields rich in stars --such as this one-- will be used for PSF characterization.

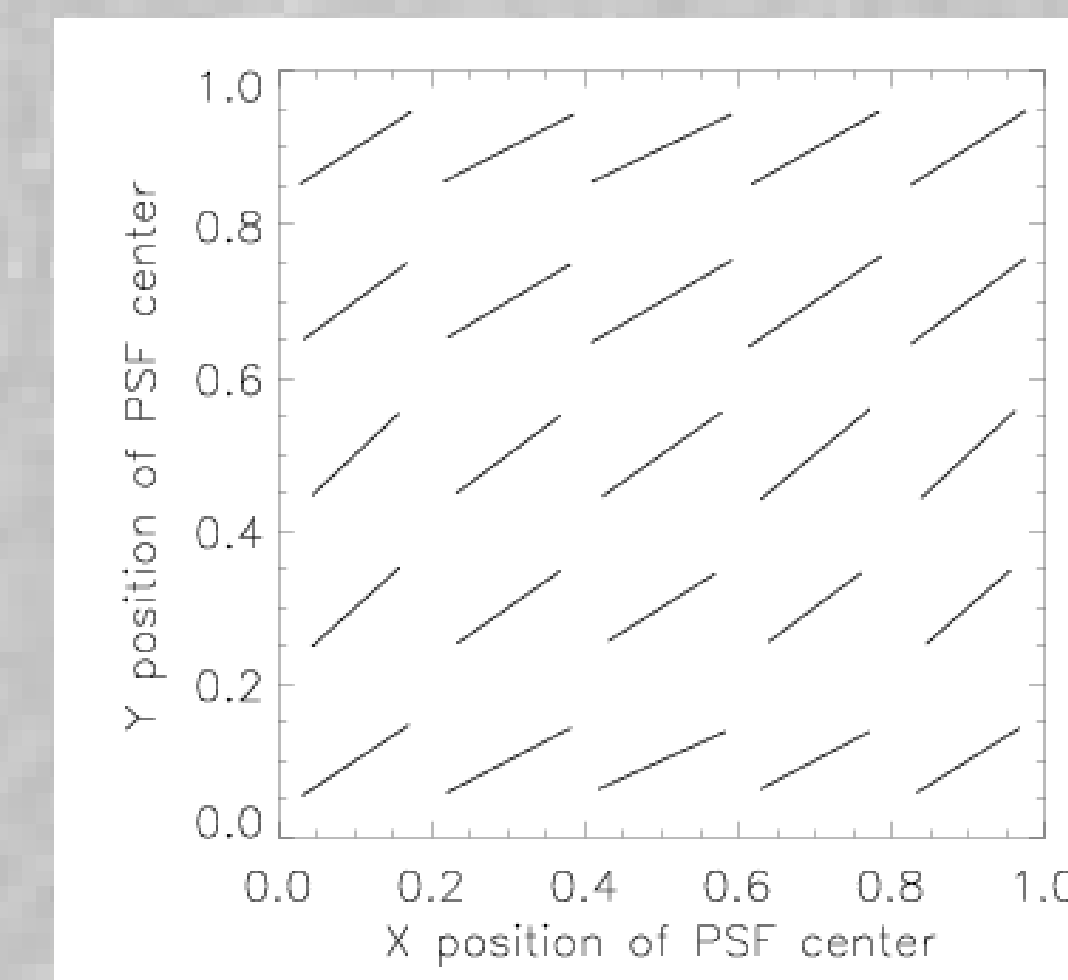


Fig. 6: Variation of ellipticity as the source center moves at the subpixel level. Ellipticity is measured for pixel (400,400) of WF3 at the nominal focus. Ellipticity values range from 0.004 to 0.063 for the $e1$ component and from 0.067 to 0.097 for the $e2$ component.

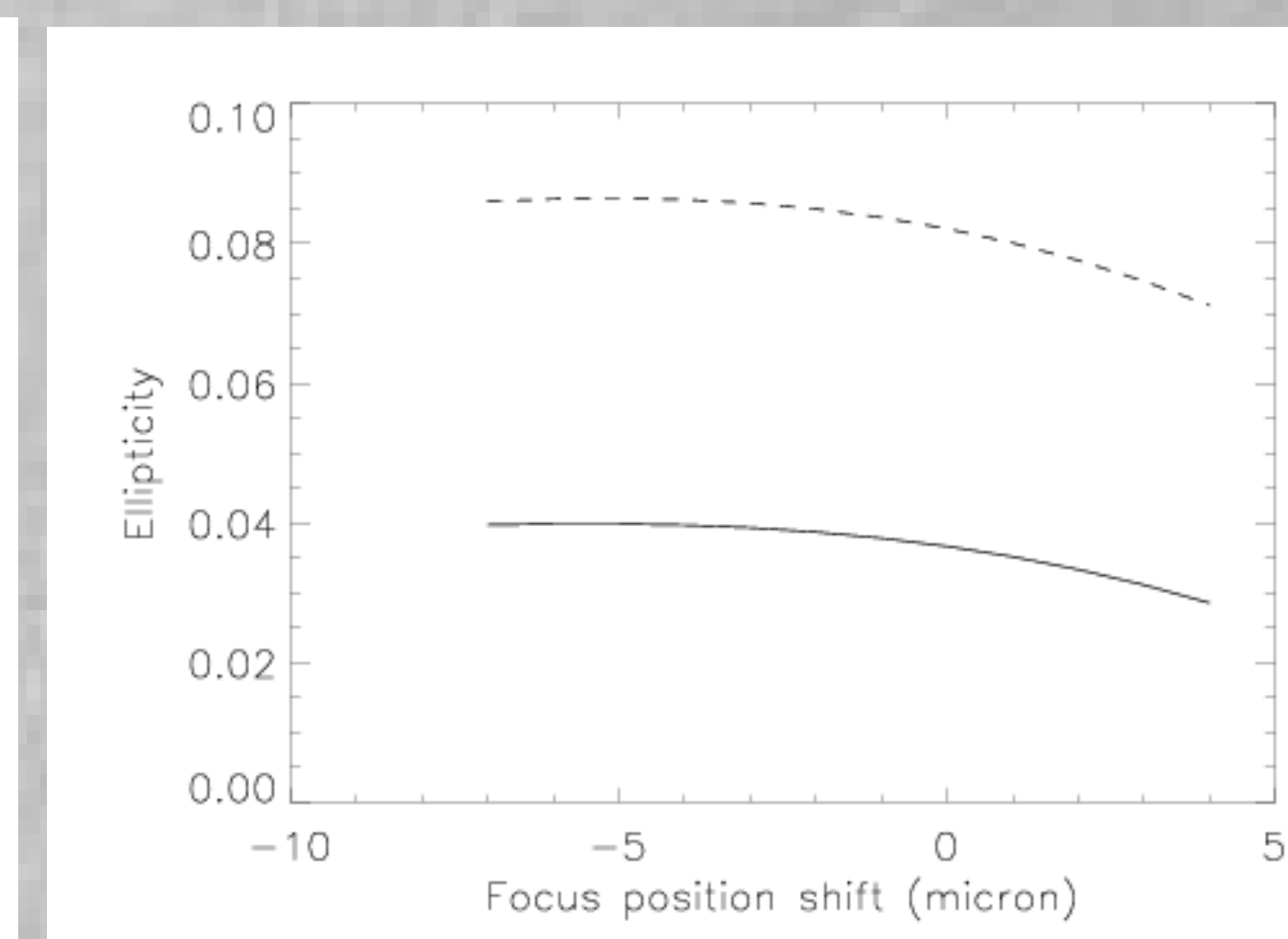


Fig. 7: Variation in measured values of ellipticity due to change in telescope focus for a PSF centered on pixel (400,400) of WF3. The $e1$ component of the ellipticity tensor is plotted as a solid line and the $e2$ component is plotted as a dashed line.

Figures 6 and 7 present a cautionary tale. Figure 6 shows how the predicted ellipticity from the TinyTim model varies as the source position moves at the subpixel level. The ellipticity variation is significant; the RMS variation of the ellipticity vector is 1.8%. Since this variation is of the same order as the cosmic shear signal we hope to measure, it cannot be discounted offhand. PSF ellipticities can be readily corrected for subpixel positioning effects; however, the potential impact on sources with complex, irregular structure (galaxies), although likely smaller, will need to be quantified using detailed simulations. Fig. 7 shows the variation in the PSF ellipticity pattern due to changes in the telescope focus, corresponding to an effective motion of the secondary mirror from -7 to +4 micron with respect to the nominal focus. This range is consistent with the variations seen historically over the period of the APPP observations; furthermore, focus variations are known to occur on time scales ranging from hours to months (Lallo et al. 2005). We will use HST engineering data, as well as sources in our data themselves, to include the effect of focus variations in our PSF shape estimates.

References: Bernstein & Jarvis, 2002 AJ, **123**, 583; Kaiser, Squires, & Broadhurst 1995, ApJ, **449**, 460; Krist, & Burrows 1995, Applied Optics, 34, 4951; Lallo et al. 2005 ISR TEL **2005-03**, Baltimore :STScI; Park et al (2004), ApJ, **600**, L159; Rhodes et al., 2000 ApJ, **536**, 79; Wadadekar et al. 2006, PASP, in press, [astro-ph/0511225](http://arxiv.org/abs/astro-ph/0511225)